A Hybrid Boundary Element Method-Reluctance Network Method for Open Boundary 3D Non Linear Problems

Douglas Martins Araujo, Jean-Louis Coulomb, Olivier Chadebec, Loïc Rondot

A Hybrid Boundary Element Method-Reluctance Network Method for Open Boundary 3-D Nonlinear Problems

Douglas Martins Araujo[1,2], Jean-Louis Coulomb[2], Olivier Chadebec[2], and Loic Rondot[1]

[1]Research and Development, Power Technology Strategy, Schneider Electric Industries SAS Grenoble, Grenoble 38050, France
[2]G2Elab, Université de Grenoble (Grenoble INP, UJF, UMR CNRS 5269), Grenoble, France

A scalar potential formulation coupling a hybrid boundary element method and a reluctance network method is presented to solve 3-D nonlinear magnetostatic problems. The computation times and the accuracy of this approach are compared with those of the finite element method in the context of force and torque evaluations. It is shown that this method could efficiently be used for the presizing of actuators. Discussion concerning the advantages of this approach compared to a pure reluctance network method is also presented.

Index Terms— Actuator modeling, boundary element method, coupled numerical methods, magnetostatics, reluctance network method.

I. Introduction

BASED on the principle of equivalent magnetic circuits, reluctance network method (RNM) is an approach that enables a very quick evaluation of electromagnetic quantities in devices [1]. Although easy to implement, RNM results can be somewhat inaccurate in a first step, especially if significant flux leakages are associated with the device. Thus, the network can be improved by comparing the results with those from the FEM model and rebuilding a more representative RNM. Unfortunately, the development of models using this approach can be very time consuming.

In fact, to be able to use RNM, a deep understanding of the device under study is needed, especially the flux paths. The magnetic flux path can easily be predicted in the regions where the permeability is high. However, in low-permeability regions—the air region, for instance—important leakage flux appears. It is exactly where the magnetic energy is greater and, thus, where a good representation of magnetic field is needed.

Tools based on FEM [2] provide the user with an effective representation of the device. Compared to RNM, in FEM the geometric and physical properties are both precisely and quickly described. Furthermore, the FEM can solve a wide range of problems. Models based on FEM need a full domain representation including magnetic nonlinear regions and the surrounding region. As consequence, the number of degrees of freedom can dramatically increase. Resolution times can be prohibitive for the actuator presizing step. This question is more worrisome in a context of optimization with a large number of parameters.

Recently, many integral formulations have been developed [3]. Integral methods can be used to represent nonlinear regions and take into account implicitly the surrounding linear region, as the volume integral methods (VIMs). A drawback of these methods is the building of a fully populated matrix. Thus, the assembly time can be prohibitive. This problem can be avoided by using compression methods [4]. Another strategy is to use them with very coarse meshes. The accuracy will then decrease, but can be acceptable in the context of presizing actuators, for instance.

In this paper, another class of integral methods known as the BEM is used to model linear unbounded regions. In this method, the degrees of freedom are located on the interface of domains (bounded and unbounded). In order to develop an efficient formulation, in terms of computational efforts and to ensure a good accuracy, a coupling between differential and integral methods seems appropriate. Furthermore, the designers would be able to add their knowledge, the flux path for example, to the model. This paper proposes a new hybrid method combining the BEM for the surrounding region (the air) and RNM for magnetic regions to take advantage of their respective merits. This approach has been already presented for 2-D applications [5], and it is now extended to 3-D problems. First, the magnetostatic problem and a quick overview of methods coupled in the new formulation (RNM and BEM) are presented. Second, the coupling is described. Finally, numerical results obtained with our approach are compared with those from FEM in order to demonstrate its efficiency.

II. Magnetostatic Problem

In order to study the distribution of magnetic quantities (such as magnetic field and induction) in a given device and neglecting temporal variations, Maxwell's equations for a magnetostatic problem are considered in Fig. 1, which are as follows:

$$\operatorname{curl} \mathbf{h} = \mathbf{j} \tag{1}$$

$$\operatorname{div} \mathbf{b} = 0. \tag{2}$$

Introducing magnets, the following relationships are valid

$$\mathbf{b} = \mu \, (\mathbf{h} - \mathbf{h_c}) \tag{3}$$

where $\mu = \mu(h)$.

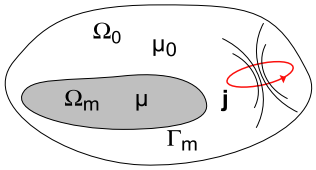

Fig. 1. Magnetostatic problems.

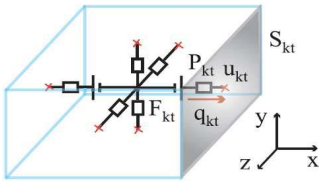

Fig. 2. Introducing NRM in the brick of the magnetic domain.

The domain will be split into several simply connected domains as a way to verify the existence of potentials [6].

Ω_m: a magnetic region that does not contain current: this region may optionally contain magnets.

Ω_0: an outside region that can accept the presence of electric currents.

As the main objective is to couple methods, it is necessary to define one or more common magnetic quantities taken from both methods. This is why we define the scalar magnetic potential

$$\mathbf{h} = -\text{grad}\ \phi. \tag{4}$$

Equations (2) and (4) are valid in the air region. Let us also define the magnetic flux, as this quantity will be useful later

$$\mathrm{q} = \int_{\mathrm{S}} \mathbf{b_n} \cdot \mathbf{n}\, \mathrm{ds} \tag{5}$$

where S is the boundary of Ω_m and $\mathbf{n}$ its external normal.

III. Boundary Element Method

Considering that there are no source fields in the free space, and using (2) and (4), the problem can be represented by a Laplacian equation. The main idea is to solve the Laplacian equation transforming the volume integral equation over all space Ω_0 into a surface integral at the boundary Γ_m. This transformation can be made making use of Green's identity.

Considering the third Green's identity applied in the air region to the scalar magnetic potential ϕ, we have

$$c\,(\mathbf{x_0})\ \phi\,(\mathbf{x_0}) = \int_{\Gamma_m} \left(\phi \frac{\partial G}{\partial \mathbf{n}} - G \frac{\partial \phi}{\partial \mathbf{n}} \right) d\Gamma \tag{6}$$

where $\phi(\mathbf{x_0})$ represents the magnetic scalar potential at point $\mathbf{x}_0$, G is the 3-D Green's function $(1/r)$, and r is the norm of a distance vector linking $\mathbf{x_0}$ and a point of the boundary. Γ_m is the boundary of the magnetic regions and c is the solid angle subtended by the boundary Γ_m.

We consider a constant distribution for the potential and its normal derivative at the border (zero-order shape function). Thanks to a point-matching approach (also called the collocation method), at each centroid of each element we get a very simple discretized expression of (6) in the matrix form

$$[\mathbf{H}\,]\,\mathbf{U}_{\mathrm{BEM}} + [\mathbf{T}]\ \mathbf{Q}_{\mathrm{BEM}} = 0 \tag{7}$$

where $\mathbf{U}_{\mathrm{BEM}}$ and $\mathbf{Q}_{\mathrm{BEM}}$ are vectors of dimension N, and $\mathbf{T}$ and $\mathbf{H}$ matrices are associated with following expressions [7]:

$$T_{ij} = \int_{\Gamma_j} \frac{G_i}{S_j\,\mu_j}\, d\Gamma, \qquad H_{ij} = c_{ij} - \int_{\Gamma_j} \frac{\partial G_i}{\partial \mathbf{n}}\, d\Gamma \tag{8}$$

where c_{ij} is null if $i \neq j$ and equals $2\,\pi$ if $i = j \cdot S_j$ is the surface of element j and μ_j its permeability. Let us notice that $\mathbf{T}$ is an invertible matrix.

Let us notice that the main idea of the terms S_j and μ_j is to transform normal derivative potential term into magnetic flux quantity.

There are many ways to perform the integration of (8) [8]. We use analytical expressions to ensure accuracy. Such analytical expressions associated with a BEM collocation method are well known.

We can write a relation linking the flux to the potential on the boundary as

$$\mathbf{Q}_{\mathrm{BEM}} = [\mathbf{P}_{\mathrm{BEM}}]\,\mathbf{U}_{\mathrm{BEM}} \tag{9}$$

$$[\mathbf{P}_{\mathrm{BEM}}] = [\mathbf{T}]^{-1}\,[\mathbf{H}]\,. \tag{10}$$

The matrix $\mathbf{P}_{\mathrm{BEM}}$ is a fully populated matrix.

IV. Reluctance Network Method

The magnetic domain is decomposed into bricks, and a reluctance network is introduced inside each of them. This element can optionally contain sources of magnetomotive force F_{kt}. Source fields could be introduced thanks to this term. A very similar coupling method linking finite elements and the reluctance network has been already presented in [9].

A. Using Reluctances to Represent a Volume Element

Let us suppose a magnetic region Ω_m discretized by K bricks. Each brick k contains T flux tubes connecting the centroid potential u_{k0} to facets. Fig. 2 represents a brick with the associated reluctances.

P_{kt} is the permeance of a flux tube and F_{kt} the magnemotive force (the way to introduce magnetomotive sources will be discussed later). q_{kt} represents the outgoing flux through the facet t of the brick k in the x-direction. u_{kt} is the averaged scalar magnetic potential of the facet k.

Using these quantities, the following relation can be written:

$$q_{kt} = (u_{kt} - u_{k0} + F_{kt})\ P_{kt} \tag{11}$$

where P_{kt} can be calculated from the permeability μ_{kt}, the length L_{kt}, and the cross section S_{kt}.

B. Flux Conservation

Combining (2) and (5), we can rewrite Gauss's law for the magnetism in terms of magnetic flux conservation as

$$\sum_{t}^{6} q_{kt} = 0. \tag{12}$$

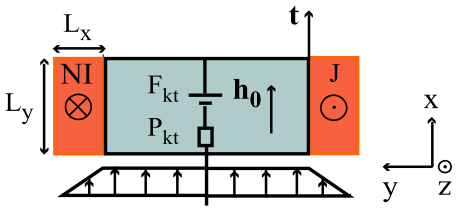

Fig. 3. Evaluating field generated by the coil.

Note that (12) allows us to impose (2) without building any tree of facets.

By isolating the central potential in (11) and considering the flux conservation, for each facet kt

$$q_{kt} = \left[\left(u_{kt} - \frac{\sum_{t=1}^{T} (u_{kt})\, P_{kt}}{\sum_{t=1}^{T} P_{kt}} \right) + \left(F_{kt} + \frac{\sum_{t=1}^{T} (F_{kt})\, P_{kt}}{\sum_{t=1}^{T} P_{kt}} \right) \right] P_{kt}. \tag{13}$$

C. Field Generated by the Coil

The magnetomotive force F_{kt} can be computed according to Ampere's law by assuming a uniform inductor field into a subset of the domain bricks. Fig. 3 shows a volume element surrounded by a coil and in which flows a current NI. L_x and L_y are the dimensions of the coil section.

Let us assume that the field $\mathbf{h}_0$ is uniform on a brick and parallel to the vector $\mathbf{t}$. Tangent to the boundary J is given by

$$J = \frac{NI}{L_y\, L_x} \mathrm{u}. \tag{14}$$

By (1), we get

$$\mathbf{h_0} \cdot \mathbf{t} = h_{0t} = \int_{L_x} J\, dx = J\, L_x = \frac{NI}{L_y}. \tag{15}$$

The field h_{0t} is independent of L_x, and we can then deduce the magnetomotive force

$$F_{kt} = \frac{NI}{L_y} L_{kt} \tag{16}$$

where L_{kt} is the length of tube t.

V. Coupling Both Methods

It remains now to couple both methods. Equation (13) can be rewritten as follows:

$$[\mathbf{Q}_{\mathrm{RNMborder}}] = [\mathbf{P}_{\mathrm{RNM}}]\, \mathbf{U}_{\mathrm{RNM}} + \mathbf{F}_{\mathrm{RNM}} \tag{17}$$

where $\mathbf{P}_{\mathrm{NRM}}$ represents the permeance matrix, $\mathbf{U}_{\mathrm{NRM}}$ the potentials, $\mathbf{Q}_{\mathrm{NRMborder}}$ the flux through the border of the device, and $\mathbf{F}_{\mathrm{NRM}}$ the magnetomotive forces created by sources. Note that $\mathbf{P}_{\mathrm{NRM}}$ is a sparse matrix, and we have more unknowns than equations.

Thanks to (9) and (17), we can easily eliminate the external flux unknowns and build a matrix representing the BEM-RNM coupling as

$$\left[\mathbf{P}_{\mathrm{BEM-RNM}}\right] \mathbf{U}_{\mathrm{RNM}} = \mathbf{F}_{\mathrm{RNM}} \tag{18}$$

where $\mathbf{P}_{\mathrm{BEM-RNM}}$ is built using $\mathbf{P}_{\mathrm{BEM}}$ and $\mathbf{P}_{\mathrm{RNM}}$ matrices.

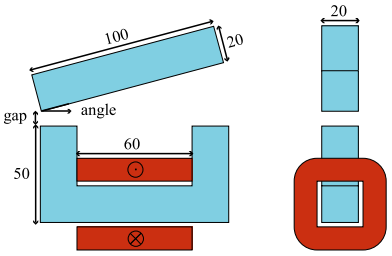

Fig. 4. 3-D U-shaped actuator. Front (left) and side (right) views are represented. The magnetic circuit is in blue and the coil is in red.

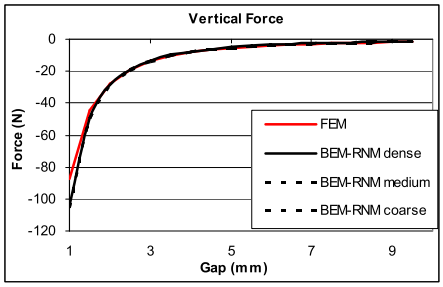

Fig. 5. Vertical force as a function of gap.

VI. Final Resolution

To apply this approach, we focus on models with coarse meshes. The number of degrees of freedom being small, an LU factorization is used to solve the linear system.

The nonlinear ferromagnetic material is represented by an initial permeability and a saturation level. The fixed-point method is used to solve the nonlinear problem. Tests have been made in order to check the convergence when the saturation point is changed. No problem of convergence was found. However, the computation time could eventually be improved by using well-known Newton–Raphson method. Once the problem has been solved, the Maxwell stress tensor approach is used to compute the forces [10]

$$\mathbf{F}_m = \oint_{\Gamma_m} \left[\frac{1}{\mu} (\mathbf{b} \cdot \mathbf{n}) \cdot b - \frac{1}{2\mu} b^2 \cdot \mathbf{n} \right] ds. \tag{19}$$

VII. Results and Comparisons

In this section, comparisons between an FEM model and our BEM-RNM model of the actuator represented in Fig. 4 are presented.

The magnetic circuit is nonlinear, and (20) represents the nonlinear characteristics using two coefficients $J_s = 2$ T and $\mu_r = 1000$

$$b(h) = \mu_0 h + \frac{2J_s}{\pi} \mathrm{arctg} \left(\frac{\pi (\mu_r - 1)\, \mu_0 h}{2J_s} \right). \tag{20}$$

In order to present the comparison, the variation of the air gap thickness and variation of the angular position of the mobile part are considered. Fig. 6 presents the force errors computed with BEM-RNM as a function of the air gap thickness in comparison to a FEM reference computed with a very dense mesh. FEM dense, FEM medium, FEM coarse, BEM-RNM dense, BEM-RNM medium, and BEM-RNM coarse represent other BEM-RNM solutions using different mesh sizes (see Table I).

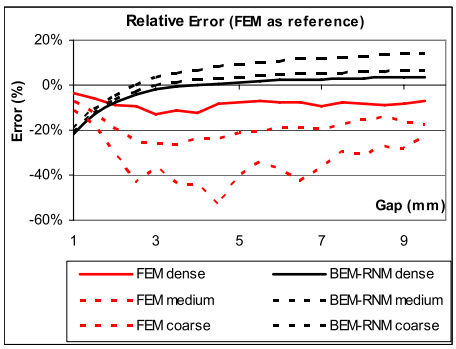

Fig. 6. Relative error as a function of gap.

TABLE I
COMPUTATION TIME

METHOD	FEM dense	FEM medium	FEM coarse	BEM RNM dense	BEM RNM medium	BEM RNM coarse
DOF	27687	9372	4522	1008	328	52
TIME (S)	770	285	97	395	28	1

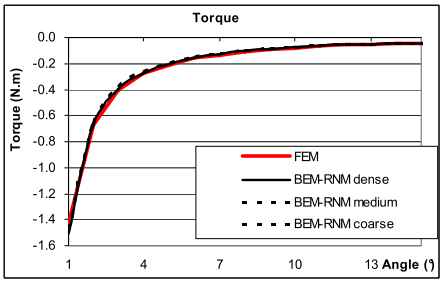

Fig. 7. Torque as a function of angle.

A. Vertical Displacement

Fig. 5 represents the evolution of the magnetic force as a function of the air gap. Results obtained with this approach seem to be very accurate even with a very coarse mesh. FEM dense mesh has been used in order to validate our approach.

The aim now is to study the variation of the accuracy with respect to the computation time. The error is divided by a reference value of force in order to get a relative one. This reference has been obtained using a very dense mesh FEM.

Twenty different positions are computed for each problem. Computation times and number of degrees of freedom are presented in the Table I. It is seen that, with FEM, mesh size cannot decrease drastically. Otherwise, the quality of the result becomes poor (see results of coarse FEM).

Inaccuracies for the BEM-RNM appear when the gap becomes too small. However, our new method remains very efficient if we consider its time consumption versus the quality of its results (see results of BEM-RNM coarse associated with 52 degrees of freedom).

B. Mobile Rotation

In this part, torque evolution as a function of angle is presented. Fig. 7 compares FEM results obtained with a very dense mesh and those obtained with BEM-RNM.

Results for both methods show good adequacy, which demonstrates the robustness of the proposed method. Good accuracy is obtained using only very few degrees of freedom.

VIII. CONCLUSION

A new formulation based on the coupling between RNM and BEM has been proposed. It has been shown that a very coarse mesh associated with a very low computation time is good enough to get quite accurate results. Getting an equivalent accuracy with FEM requires much more computation time. To build RNM models for systems with rotating motion could be a very hard job, and the accuracy of results is usually poor.

The process of presizing electromagnetic actuators needs a fast, accurate, and robust method. Engineers do not have sufficient time for long but accurate calculations proposed by FEM. The building of an RNM model can also take very long and often requires specific expertise. Sometimes, the FEM is used to study the behavior of leakage flux before building an RNM model, leading to difficult iterations between both numerical methods.

Today, another relation connecting accuracy, computational effort, and time to develop the model is needed. The proposed method is a good compromise between these three requirements.

By considering that optimization is an important tool for presizing actuator, new opportunities could be provided with the presented method. In the context of numerical model optimizations, computation times can be prohibitive. With this new approach, more accurate results could be obtained without increasing dramatically the time of presizing.

REFERENCES

[1] B. du Peloux, L. Gerbaud, F. Wurtz, V. Leconte, and F. Dorschner, "Automatic generation of sizing static models based on reluctance networks for the optimization of electromagnetic devices," *IEEE Trans. Magn.*, vol. 42, no. 4, pp. 715–718, Apr. 2006.

[2] J.-L. Coulomb, "Finite elements three dimensional magnetic field computation," *IEEE Trans. Magn.*, vol. 17, no. 6, pp. 3241–3246, Nov. 1981.

[3] A. Carpentier, O. Chadebec, N. Galopin, G. Meunier, and B. Bannwarth, "Resolution of nonlinear magnetostatic problems with a volume integral method using the magnetic scalar potential," *IEEE Trans. Magn.*, vol. 49, no. 5, pp. 1685–1688, May 2013.

[4] L. Greengard and V. Rokhlin, "A fast algorithm for particle simulations," *J. Comput. Phys.*, vol. 73, no. 2, pp. 325–348, Dec. 1987.

[5] D. Martins Araujo, J.-L. Coulomb, B. Delinchant, and O. Chadebec, "A hybrid method BEM-NRM for magnetostatics problems," in *Proc. MOMAG*, Oct. 2012, pp. 1–14.

[6] J. Simkin and C. W. Trowbridge, "Three-dimensional nonlinear electromagnetic field computations, using scalar potentials," *Electr. Power Appl.*, vol. 127, no. 6, pp. 368–374, 1980.

[7] C. A. Brebbia, *The Boundary Element Method For Engineers*. Mountain View, CA, USA: Pentech Press, 1984.

[8] C. Rubeck, J. Yonnet, H. Allag, B. Delinchant, and O. Chadebec, "Analytical calculation of magnet systems: Magnetic field created by charged triangles and polyhedra," *IEEE Trans. Magn.*, vol. 49, no. 1, pp. 144–147, Jan. 2013.

[9] A. Demenko, L. Nowak, and W. Szelag, "Reluctance network formed by means of edge element method," *IEEE Trans. Magn.*, vol. 34, no. 5, pp. 2485–2488, Sep. 1998.

[10] Z. Ren and A. Razek, "Force calculation by Maxwell stress tensor in 3D hybrid finite element-boundary integral formulation," *IEEE Trans. Magn.*, vol. 26, no. 5, pp. 2774–2776, Sep. 1990.